

A detailed assessment of snow accumulation in katabatic wind areas on the Ross Ice Shelf, Antarctica

David A. Braaten

Department of Physics and Astronomy, University of Kansas, Lawrence

Abstract. An investigation of time dependent snow accumulation and erosion dynamics in a wind-swept environment was undertaken at two automatic weather stations sites on the Ross Ice Shelf between January 1994 and November 1995 using newly developed instrumentation employing a technique which automatically disperses inert, colored (high albedo) glass microspheres onto the snow surface at fixed intervals throughout the year. The microspheres act as a time marker and tracer to allow the accumulation rate and wind erosion processes to be quantified with a high temporal resolution. Snow core and snow pit sampling was conducted twice during the study period to identify microsphere horizons in the annual snow accumulation profile, allowing the snow accumulation/erosion events to be reconstructed. The two sites chosen for this investigation have characteristically different mean wind speeds and therefore allow a comparative examination on the role of wind on ice sheet growth. Mass accumulation rate at the two sites for the 14-day integration periods available ranged from 0.0 to $>2.0 \text{ kg m}^{-2} \text{ d}^{-1}$. The mean mass accumulation rate during the study period was greater at the site with stronger winds ($0.69 \text{ kg m}^{-2} \text{ d}^{-1}$) than the site with lower mean wind speeds ($0.61 \text{ kg m}^{-2} \text{ d}^{-1}$); however, the difference between the two means is not statistically significant. Accumulation rates derived from an ultrasonic snow depth gauge operated at one of the sites are compared to the actual tracer-derived accumulation rates and show the limitations of only having a measure of snow surface height with no instantaneous measurements of the snow density profile. Snow depth gauge derived accumulation rates were found to be greatly overestimated during high-accumulation periods and were greatly underestimated during low-accumulation periods.

1. Introduction

Polar ice sheets are an important component of the global climate system; however, their remote and harsh environment confound and limit experimental attempts to understand their dynamics and interactions with the atmosphere and oceans. Polar ice sheets contain approximately 2% of the Earth's water and therefore negative changes in ice sheet mass balance can potentially have serious implications due to a rise in global sea level, although it is still an open question whether polar ice sheets grow or decay under a warming climate scenario [Jacobs, 1992]. Polar ice sheets are also valuable archives of direct and indirect evidence of millennial-scale climatic events and past atmospheric composition of trace gases and aerosols. Proper interpretation of this evidence requires a thorough knowledge of the dynamical processes which govern ice sheet growth.

Processes which control local ice sheet changes can be categorized in terms of source and loss parameters. Source parameters include episodic snowfall events associated with synoptic scale features such as cyclones and fronts [Bromwich, 1988] and hoar frost deposition. Loss parameters include sublimation [Fujii and Kusunoki, 1982] and snow erosion caused by drifting or blowing snow; however, snow grains removed by erosion may be replaced by snow which has eroded from upwind locations. The process of snow erosion is

complex and has been examined experimentally by Budd *et al.* [1966], Kobayashi [1978], Wendler [1989], and Maeno *et al.* [1995] using innovative experimental techniques to examine various characteristics such as mass flux and snow grain size as a function of height and wind speed. Naturally, these processes can only occur when the wind speed exceeds some threshold speed for snow grain movement (saltation), which usually depends on the condition of the snow surface. Age-hardened snow has a much higher threshold saltation speed than recently deposited snow. Bromwich [1988] gives a range of threshold speeds between 7 and 13 m s^{-1} ; however, during this study the saltation threshold wind speeds on the Ross Ice Shelf were observed to be between 5 and 6 m s^{-1} . Wind movement of surface snow results in a variety of different surface features which have been classified as depositional and/or erosional patterns by Kobayashi and Ishida [1979]. They conclude that wind speeds less than 15 m s^{-1} (at 1 m above the surface) produce transverse features such as ripples, waves, and barchans, whereas wind speeds greater than 15 m s^{-1} produce longitudinal features such as dunes and sastrugi. The microphysical processes which produce these features are complex, and essentially nonlinear, in that the turbulent airflow distorts the snow surface which in turn distorts the flow. External characteristics such as amplitude, wavelength, shape, and movement have been examined by Budd *et al.* [1966] and Kobayashi and Ishida [1979]; however, important aspects such as snow grain transport and mixing into the accumulation profile remain largely unknown. Since most precipitation events at the coastal margins of Antarctica are associated with wind speeds greater than the threshold speed

Copyright 1997 by the American Geophysical Union.

Paper number 97JD02337.
0148-0227/97/97JD-02337\$09.00

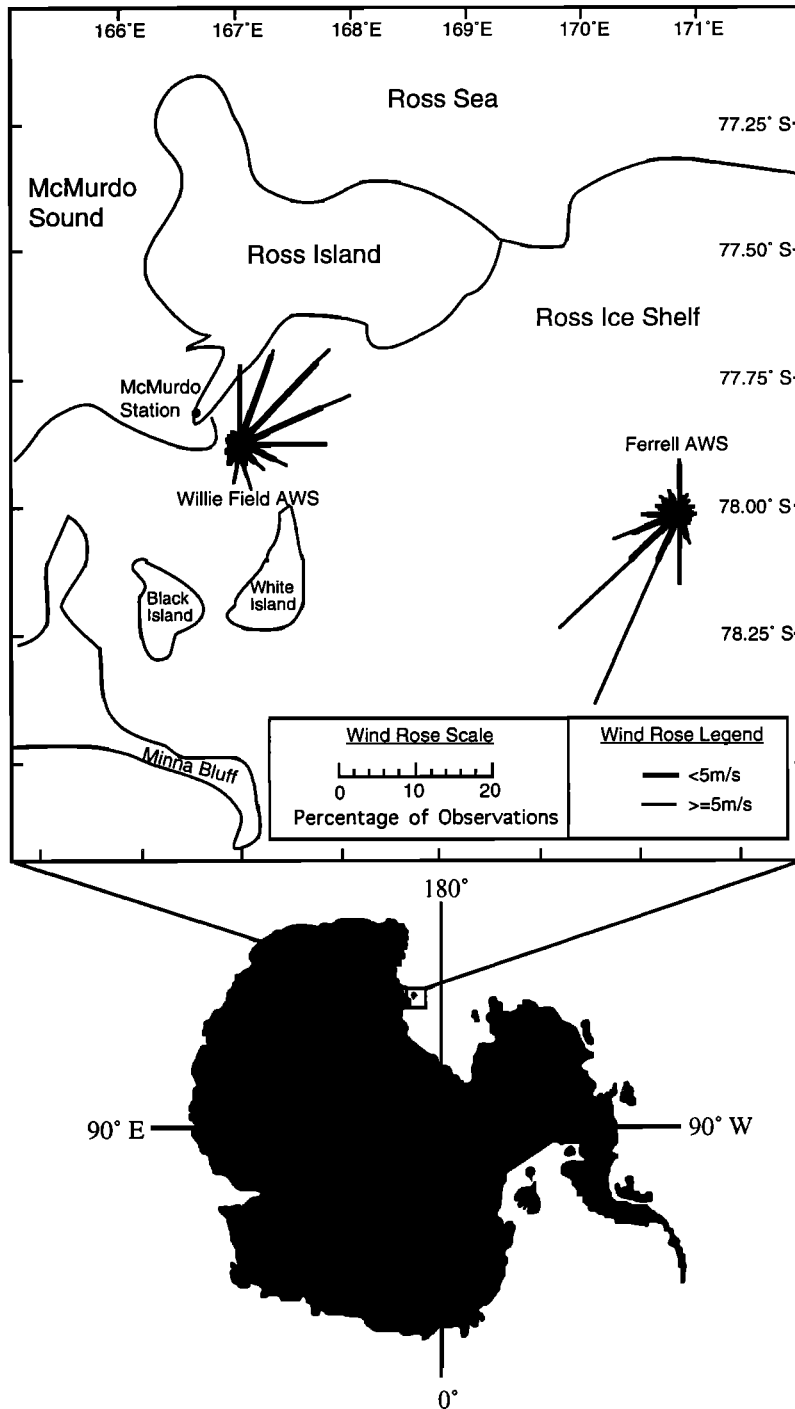


Figure 1. Location of automatic weather stations where snow accumulation experiments were conducted. Wind roses summarize the winds during the study period, showing the prevailing directions from which the winds were coming.

for blowing snow, source and loss parameters are interrelated in that layers of accumulated snow are generally a mixture of snow produced by individual storms and from previous storms which has been eroded and transported from upwind locations [Bromwich, 1988].

This investigation was conducted to obtain greater quantitative insight into the time dependent processes of ice sheet snow accumulation in windswept areas. Experiments were carried out at two locations on the Ross Ice Shelf using a

new automated system to disperse colored glass microspheres onto the snow surface at preset time intervals to act as a tracer. These sites are Willie Field automatic weather station (AWS) (77.85°S, 167.08°E) located approximately 10 km east of McMurdo Station (MCM) and Ferrell AWS (78.02°S, 170.80°E) located approximately 100 km east of MCM (Figure 1). Evaluation of snow accumulation at each site was conducted in two phases between January 1994 and November 1995. For the Willie Field AWS the two evaluation periods

were January 18, 1994, to January 28, 1995, and February 1, 1995, to November 2, 1995, and for the Ferrell site the evaluation periods were January 25, 1994, to January 21, 1995, and January 25, 1995, to November 17, 1995.

2. Wind and Precipitation Characteristics

2.1. Automatic Weather Stations

The two AWS sites used in this study are part of a large array of stations deployed on the continent [Holmes *et al.*, 1996]. Each AWS provides 10 min measurements of air temperature, wind speed and direction, atmospheric pressure, relative humidity, and vertical differential temperature (2 m) transmitted to polar-orbiting satellites, although between 15% and 20% of the measurements are intermittently lost because a satellite is not in position to receive the broadcast. Data are collected through the Argos Data Collection and Location System (ARGOS) and processed by Space Science and Engineering Center, University of Wisconsin-Madison [Stearns and Wendler, 1988]. Since both AWS sites are located where annual snow accumulation is approximately 0.5 m yr^{-1} , the height of the wind speed measurement at both sites decreased from ~ 3 to ~ 2 m during the study period. The two study sites have characteristically different wind regimes, although both sites experience katabatic winds and are close enough to be influenced by the same synoptic scale storms. Figure 1 provides wind roses for each AWS, summarizing the wind observations during the entire study period. Winds at Willie Field AWS are moderated by the proximity to topographic features of Ross Island, White Island and Black Island, with 21.2% of the observations exceeding 5 m s^{-1} (approximate snow grain saltation threshold) and prevailing directions for winds with speeds greater than 5 m s^{-1} ranges between 60° and 210° . It is not unusual for wind speeds at Willie Field to exceed 15 m s^{-1} during katabatic wind outflow events in which prevailing wind directions are mainly between 160° and 210° . Winds at Ferrell are strongly influenced by moderate katabatic outflow winds with 44.1% of the observations exceeding 5 m s^{-1} and a dominant wind direction

corridor from 210° with a directional standard deviation of 18.5° for wind speeds $> 5 \text{ m s}^{-1}$.

At Willie Field only, a Campbell Scientific ultrasonic snow depth gauge and CR10 data logger with a data storage module supplements the AWS data, providing hourly measurements of distance to the snow surface with an accuracy of ± 10 mm. These data were retrieved once per year. For most days, more than 90% of these hourly measurements are valid. Occasionally, erroneous data were recorded for several consecutive days which was most likely due to ice crystal buildup (hoar frost) on the sensor housing. In 1994, data were missing from 23% of the days with the longest consecutive period being 30 days, and 22% of the days in 1995 were missing with the longest consecutive period being 20 days. Figures 2a and 2b give the daily average snow depth gauge derived accumulation during the study period at Willie Field. These data show both large positive and negative accumulations on short timescales with a substantial long-term positive accumulation. Positive changes are associated with precipitation, wind blown transport of snow into the target area, and/or the formation of a surface feature on the target area. Negative changes can result from wind erosion, sublimation, gravitational forces which compact the snow, and metamorphic processes of the snow crystals [Colbeck, 1983]. Figure 2a corresponds to the period before the first field evaluation of snow accumulation processes, and Figure 2b represents the period before the second field evaluation.

2.2. McMurdo Station Precipitation Observations

Daily precipitation summaries from McMurdo Station derived from individual observations of trained weather observers were obtained for the entire study period with the exception of August 1995 which was not available. Quantifying snowfall accumulation is difficult in the windswept Antarctic environment and is usually estimated based on intensity of precipitation and duration. The bars in Figures 2a and 2b identify when precipitation episodes occurred and the estimated accumulation amount. Not included

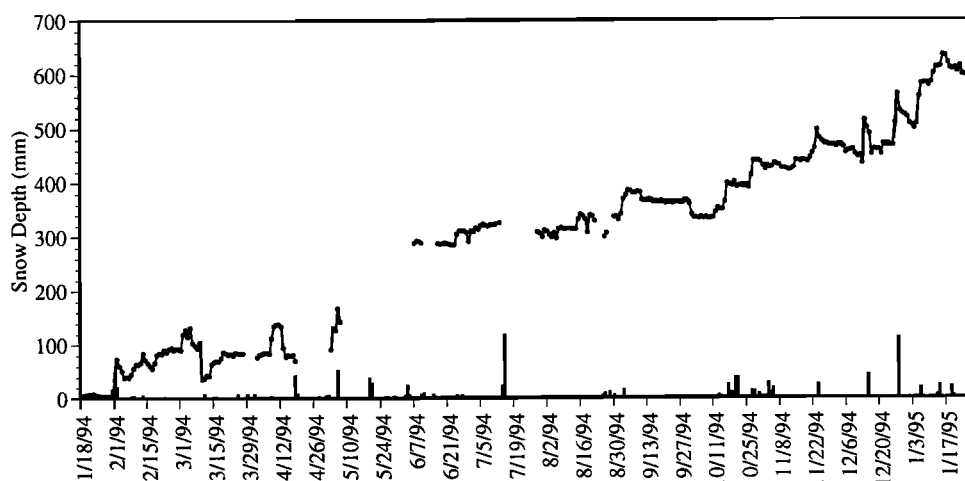


Figure 2a. The connected data points show the daily average snow depth at Willie Field obtained from an ultrasonic snow depth gauge from the start of the field experiment until the first field survey on January 28, 1995. The vertical bars along the time axis show precipitation amounts reported at McMurdo Station. The dates given on the time axis are the planned microsphere activations at Willie Field.

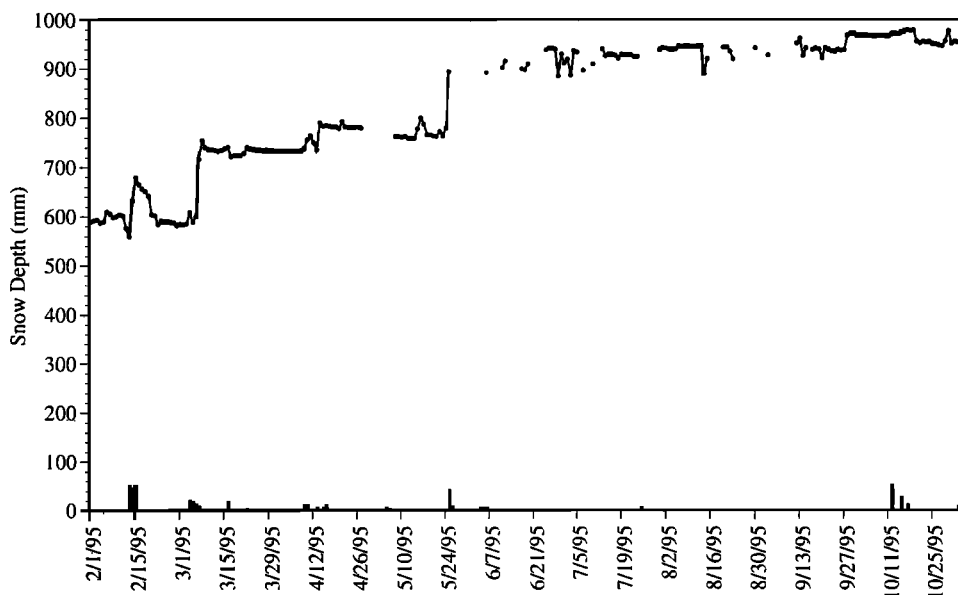


Figure 2b. Same as Figure 1a, except for the second field period between February 1, 1995, and November 2, 1995.

are the 245 days in which trace snowfall amounts (<1.3 mm) were reported. A total of 55 precipitation episodes occurring over one or more days are shown, with 16 episodes occurring during periods in which the snow depth gauge data were missing. While most of the positive snow accumulation changes indicated by the snow depth gauge were associated with a precipitation episode, only 18 of the precipitation episodes were associated with a corresponding positive change in snow accumulation greater than the accuracy of the snow depth gauge. As for the remaining 21 precipitation events in which the snow depth gauge does not indicate a corresponding change in snow surface height, explanations for this include the possibility that the observed precipitation was localized, the precipitation resulted in a local accumulation which was less than the accuracy of the snow depth gauge, or that moderate to strong winds restricted the accumulation since the vast majority of these events were associated with wind speeds >5 m s^{-1} .

3. Detailed Characterization of Snow Accumulation

3.1. Microsphere Dispersal System

To allow dating of snow accumulation horizons and to assess the role of wind on accumulation dynamics at the two AWS sites, colored glass microspheres (with a high albedo) were dispersed onto the snow surface periodically throughout the study period as time markers within the growing ice sheet, and as a tracer to quantify snow grain mixing and transport processes. A similar idea was used in earlier studies of wind-blown sand surfaces by *Hunter* [1977] who periodically sprinkled a small amount of dark magnetite grains on a blowing sand surface to record the internal structure of the sediment bed to successive deposition of sand grains. Automated dispersal of the 120 μm diameter glass microspheres (density = 2.5 g cm^{-3}) was accomplished by instrumentation referred to as the microsphere dispersal system (MDS) [Braaten, 1994, 1995] which consists of three

aerosol generator units mounted on aerodynamic masts and a pneumatic system (buried ~ 1.5 m below the snow surface) controlled by a microcontroller-based timing system to activate the aerosol generators and disperse the microspheres. The MDSs at both sites were programmed to activate every 14 days for 10 s, dispersing ~ 75 mL of the inert, colored microspheres from a height of ~ 1.2 m. The microspheres have a terminal settling speed of 0.9 m s^{-1} and rapidly fall to the snow surface. A total of four different colors (pink, green, orange, and yellow) are used by MDS, each dispersed during successive 14 day periods; therefore any given microsphere color is dispersed in a 56 day cycle. At the start of each field evaluation period, yellow flat glass shards (150 to 425 μm) are dispersed by hand onto the snow surface to allow an unambiguous identification of the base of the accumulation layer.

Performance of MDS during the first field period was evaluated based on a forensic examination of system components, volume of microspheres remaining in the aerosol generator units and a snow core site survey. For the second field period, pressure transmitters were added to the pneumatic system and system pressure recorded hourly by Campbell Scientific CR10 data loggers. Ambient temperature of the pneumatic system was also recorded by the CR10 once per day. Pneumatic system pressure provides a log of microsphere dispersal activations by confirming an activation occurred or indicating a system failure and allows an accurate estimate of the volume of microspheres dispersed to be made based on the magnitude of the system pressure change. For each confirmed activation, the AWS at each site provided wind speed and wind direction measurements within a few minutes of each MDS activation, allowing an accurate estimation of where the microspheres were deposited. Figure 3 provides site maps of each MDS site during each deployment and indicates the direction from which the winds were coming and wind speed (proportional to the length of the line) during each confirmed activation. During the study period a total of 45 and 46 MDS activations were planned for Willie Field and Ferrell,

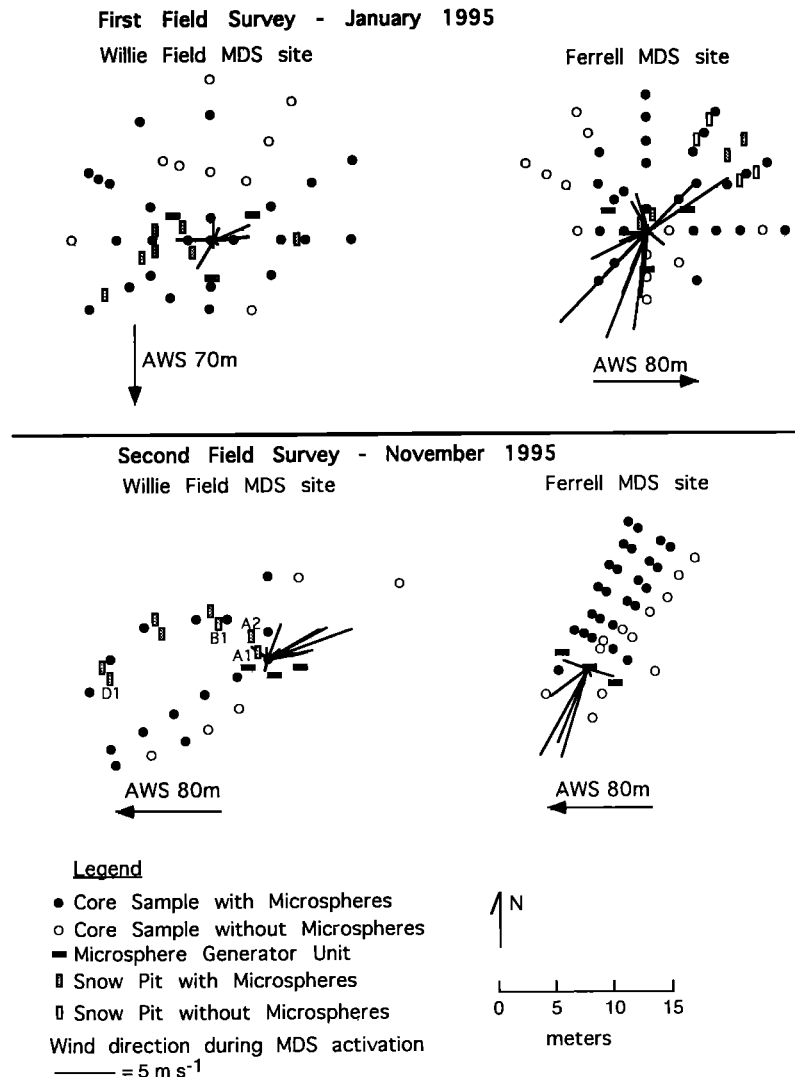


Figure 3. Site maps for each field sampling campaign at Willie Field and Ferrell showing locations of microsphere generators, snow cores, snow pits, and the wind speed and direction the wind was coming from during confirmed microsphere activations.

respectively, with an actual percentage of successful activations being 47% for Willie Field (21 activations) and 52% for Ferrell (24 activations). This does not include the manual dispersals of glass shards at the beginning of each field evaluation period at each site. Figure 4 shows when each successful activation occurred and when a planned activation did not occur due to a malfunction. All system malfunctions were attributed to the gas pressure regulators of the pneumatic system; however, the MDS pneumatic system is designed using two gas pressure regulators such that if one malfunctions, microsphere dispersals will continue at 28 day intervals instead of the normal 14 day intervals. Pressure regulation failures were manifest as either reduced pressure downstream resulting in a large reduction in gas flow rate during activation or high pressure downstream locking the solenoid valves in the closed position. These problems were found to occur when pneumatic system ambient temperatures reached approximately -30°C despite a minimum operating temperature rating of -40°C for these regulators. This problem was discovered at the end of the first field survey in January 1995, but due to the tight field schedule, we were only

able to rebuild and test these regulators before deploying them for the second field survey. As can be seen in Figure 4, the second field survey had about the same failure rate as the first.

3.2. On-Site Snow Sampling

Reconstruction of the time dependent snow accumulation processes occurring during each survey period is based on observed vertical and horizontal spatial distribution of the colored glass microspheres, the dates of successful microsphere dispersals, and on-site meteorological data. The initial deposition location of microspheres from each activation is initially estimated using the AWS wind speed and direction observations at the time of activation (Figure 3) and a known microsphere distribution under calm conditions [Braaten, 1995]. At the conclusion of each field survey period, snow core sampling and snow pit sampling is conducted at each site with the snow samples kept frozen and returned to a laboratory in the Crary Science and Engineering Center at MCM for microsphere identification. Laboratory protocols for identification of microspheres include melting each sample, filtering all material from the meltwater, and

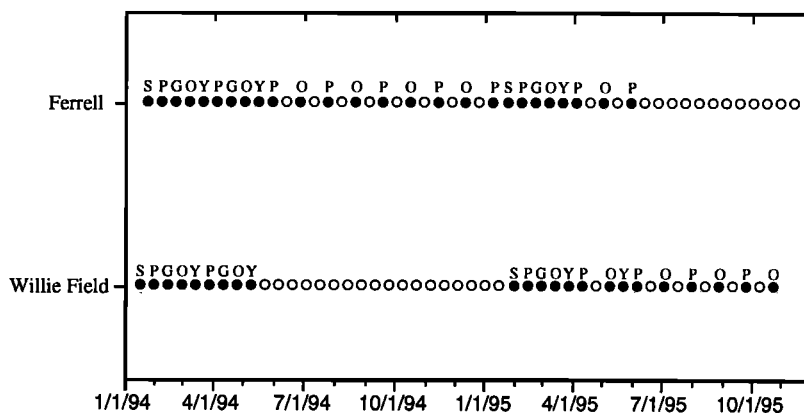


Figure 4. Microsphere activation schedule at Willie Field and Ferrell for dispersal of yellow glass shards (S), pink microspheres (P), green microspheres (G), orange microspheres (O), and yellow microspheres (Y). The solid circles indicate a successful system activation, and open circles indicate the system did not activate as planned due to a malfunction.

examining the filter media with a low-power dissecting microscope, noting the number and color of microspheres present, if any. Using these procedures, it is routine to identify a single microsphere in any given snow sample.

3.3. Snow Cores

Snow cores 0.8 m in length and 0.0045 m² in cross-sectional area were taken from the study sites with a Sipre auger. These samples provide an overview of the on-site microsphere spatial distribution integrated over the entire accumulation period and are compared to an expected distribution obtained using wind speed and wind direction data from the time of dispersal to identify possible wind erosion events. Figure 3 shows the locations of these site survey snow cores obtained during the study period. Microspheres were found in 71% of these snow cores, and Table 1 summarizes the cores collected at each site during each survey period and the microspheres identified. Also shown in parentheses are the number of confirmed activations for each color. In general, with fewer activations of a given color, a smaller number of survey cores contained microspheres with that color. This is consistent with expectations since the microsphere deposition area of each aerosol generator is typically less than 10 m² [Braaten, 1995] and the snow core surveys cover an area which varies between 150 and 400 m². For two periods with the same or nearly the same number of activations (Willie Field, period 2, pink and orange, and Ferrell, period 1, pink and orange), large differences in microsphere spatial distribution were found. To explain these differences, wind characteristics during microsphere activations were examined. In the first case, five dispersals each of pink and orange microspheres at Willie Field during survey period 2 resulted in a large fraction of cores with pink microspheres, but a small fraction of cores with orange microspheres (Table 1). During the pink microsphere dispersals, wind direction varied by 126°, whereas wind direction during orange microsphere dispersals were all within a surprisingly narrow 24° sector which explains why these microspheres were found in such a small fraction of the survey cores. In the second case, seven dispersals of pink and six dispersals of orange microspheres at Ferrell during period 1 resulted in a similar discrepancy; however, this time, wind

directions were very similar during dispersals of both pink and orange microspheres. A possible cause of this discrepancy is the occurrence of wind erosion soon after dispersal of the orange microspheres. To test this hypothesis, average wind speeds were calculated for 24, 48, 72, 96, and 120 hour periods after each confirmed microsphere dispersal, and these results were grouped by microsphere horizons positively identified by snow pit sampling and those which were not. The green and yellow microsphere dispersal events (two each) were excluded from the analysis because these microsphere colors were identified in snow core analyses but not in snow pit analyses, and therefore it is unknown which dispersal(s) the recovered microspheres are associated. The mean of each group was calculated for each of the five time periods and a *t* test was employed to assess whether the two group means were statistically different at the 0.05 level of significance. These results are shown in Table 2 and support this wind erosion hypothesis. For all averaging periods the mean wind speeds associated with the identified horizons are less than the

Table 1. Summary of Sipre Snow Cores Obtained and the Fraction of Cores Which Contain a Particular Microsphere Color

Survey Period	Cores Extracted	Fraction of Cores With Microspheres			
		Pink	Green	Orange	Yellow
<i>Willie Field</i>					
1	34	0.41 (2)	0.44 (2)	0.15 (2)	0.18 (2)
2	20	0.70 (5)	0.17 (1)	0.30 (5)	0.05 (2)
<i>Ferrell</i>					
1	40	0.63 (7)	0.10 (2)	0.10 (6)	0.13 (2)
2	25	0.56 (3)	0.04 (1)	0.16 (2)	0.00 (1)

The number of activations for a particular microsphere color are given in parentheses.

Table 2. Group Mean Wind Speeds for 24, 48, 72, 96, and 120 Hour Periods After Confirmed Microsphere Dispersal Events During the First Study Period at Ferrell.

Time After Dispersal, hours	Mean Wind Speed, Identified Horizons, m s^{-1}	Mean Wind Speed, Missing Horizons, m s^{-1}	Statistically Different Means? (0.05 Level of Significance)
24	3.38	5.71	No
48	3.82	6.69	No
72	3.52	6.47	Yes
96	3.86	5.95	Yes
120	4.05	5.69	No

Data were grouped based on whether microsphere horizons were identified or not during site sampling. A *t* test at the 0.05 level of significance was performed to determine whether the group means for each time period were statistically different.

missing horizons; however, only the 72 and 96 hour averaging periods have differences which are statistically significant. These results on the fate of newly deposited microspheres also offer insights into the mobility of snow grains after snowfall events, in that high wind speeds (exceeding the saltation threshold) occurring during a period ~4 days after new precipitation causes significant downwind transport of snow grains. If wind speeds remain low during this period, the new precipitation has a chance to age sufficiently and become resistant to wind erosion.

3.4. Snow Pits

Snow pit sampling provides high-resolution information of microsphere horizons, allowing a detailed reconstruction of the time dependent snow accumulation to be made. Snow pit locations were chosen based on winds during microsphere dispersals (Figure 3), prevailing winds (Figure 1), and the results of the snow core survey (Figure 3). Snow samples are collected in disposable cuvette sampling tubes ($1 \text{ cm}^2 \times 4.5 \text{ cm}$) which are pushed into the snow pit wall. A custom built snow pit sampling apparatus, shown in Figure 5, is used to rapidly obtain accurately positioned, high-resolution (1 cm depth) snow pit samples. The apparatus holds five cuvette tubes at a time, which are guided into the snow pit wall to extract snow samples. A bubble level on the apparatus ensures exact vertical alignment, and prepositioned sampling locations in both vertical and horizontal axes with known spacing accurate to $\sim 0.05 \text{ mm}$ allow an entire 0.5 m snow pit profile to be sampled after making a single sample tube depth measurement. The depths of subsequent sample tubes are calculated based on the reference tube depth, the sample tube number (1 through 5) and the apparatus position. Most microsphere horizons sampled were found in only one sample tube indicating that the microspheres stayed within a layer less than 1 cm in depth and therefore did not migrate vertically after deposition to the surface. The vertical mixing of microspheres which did occur was attributed to wind-generated

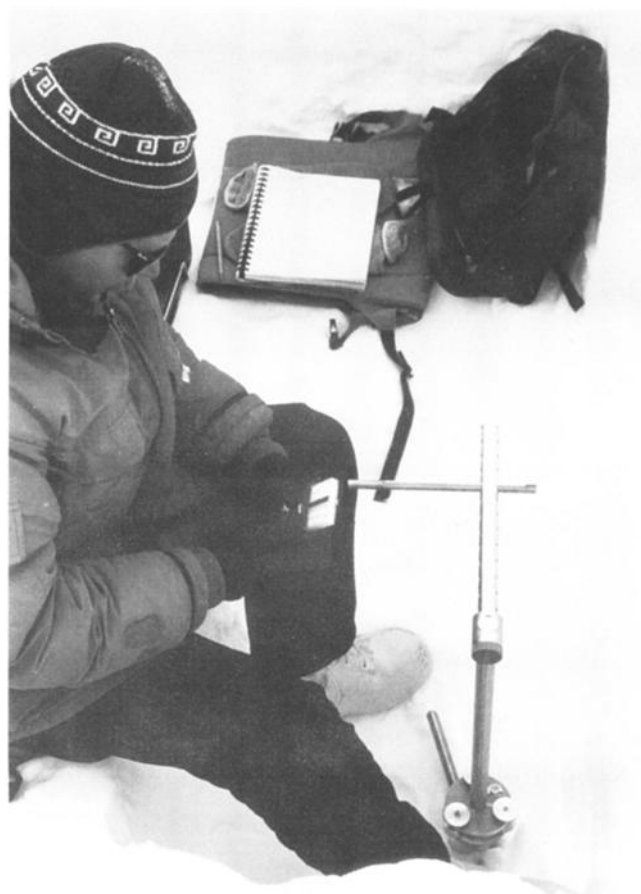


Figure 5. Collecting snow samples in cuvette tubes from a snow pit wall using an apparatus which ensures exact vertical alignment from a bubble level on the base.

surface features. High-resolution measurements of snow density were also obtained from the cuvette samples by measuring the volume of snow and the volume of water in the cuvette after melting.

Table 3 summarizes the high-resolution snow pit samples obtained at each site giving the number of snow pit profiles, the number of cuvette samples, and the fraction of samples which contained either microspheres or glass shards. Because of persistent high winds during the second Ferrell site visit, no snow pit profiles were obtained. Instead, 12 additional

Table 3. Summary of High Resolution of Snow Pit Samples and the Percentage of Cuvette Samples Containing Microspheres or Shards

Survey Period	Number Profiles	Number Samples	Percentage With Microspheres or Shards
<i>Willie Field</i>			
1	7	440	6.1
2	10	470	6.0
<i>Ferrell</i>			
1	7	495	4.4

Sipre snow cores were extracted. These cores were cut into 156 samples 3 to 4 cm in length and analyzed for microspheres and snow density. The percentage of core sections which were found to have microspheres or shards was 20.5%. This much larger recovery fraction compared to the cuvette samples is due to the greater volume of snow analyzed (by a factor of ~40); however, the vertical resolution is reduced and the uncertainty in the vertical position is increased.

3.5. Snow Horizon Dating

A "snap shot" of snow accumulation variability was determined for each study period at each site based on the depth of the glass shards scattered over the dispersal area at the start of the period, several snow stakes positioned around the dispersal area and the AWS snow depth gauge (Willie Field AWS only). Snow pit sampling at the end of the first study period at Willie Field failed to identify the glass shard horizon, but the first microsphere horizon from February 1, 1994, indicated an accumulation of $520. \pm 18$ mm, and the snow depth gauge measurement located 70 m south of the dispersal area gave an accumulation of 558 mm for this same period. Snow stakes positioned 30 m north, west and east of the dispersal area provided an accumulation measurement of $424. \pm 42$ mm for a period beginning 2 weeks earlier on January 18, 1994. During the second period the glass shard horizon was identified and indicated an accumulation of $363. \pm 15$ mm, with the snow depth gauge located 80 m west, measuring an accumulation of 367 mm. Snow stakes located 30 m north, south, east and west of the dispersal area provided an accumulation measurement of $354. \pm 17$ mm. At Ferrell during the first period, the glass shard horizon indicated an accumulation of 655 ± 5 mm, while an array of snow stakes located 30 m north, south, east and west of the dispersal area gave an accumulation of $539. \pm 29$ mm. During the second period, the glass shard horizon indicated an accumulation of 363 ± 16 mm, while a similar array of snow stakes as the first period gave an accumulation of $373. \pm 41$ mm. Snow accumulation results at Willie Field AWS show a consistently good relationship between the microsphere dispersal area and the snow depth gauge; however, the snow stake agreement at both sites is mixed. This probably results from the small number of snow stakes deployed as compared to other snow stake arrays [Mosley-Thompson *et al.*, 1995].

For a more detailed look at the snow accumulation process within the dispersal area, the microsphere horizons identified in the snow pits were used. Assigning dates to microsphere horizons identified is not a simple process, since not all microsphere horizons are found during snow pit sampling (even though they might be found during the snow core survey) and the local snow surface height can vary by several centimeters due to the intermittent presence of surface features (e.g., ripples and sastrugi). Therefore horizons of the same microsphere color found at slightly different depths in two different snow pit profiles are not necessarily from different dispersal events, and conversely, the same color microspheres found at roughly the same depth might actually be from different dispersal events. To overcome this inherent uncertainty in dating microsphere horizons, the vertical snow density distribution and the depth of visually observed ice layers were used to normalize the depth of microsphere horizons to a reference snow pit profile. The primary consideration in choosing the reference profile was identification of the glass shard horizon indicating the start of

the survey period, but if this horizon was not identified at the site, the profile with the greatest number of identified microsphere horizons was designated as the reference profile. No attempt was made to match an entire accumulation profile with the reference profile since local accumulation is often influenced by formation and movement of surface features resulting in different relative accumulation rates throughout the study period.

A good example of how microsphere data from several snow pit profiles can be normalized, and how variation in accumulation rates during the year can be identified at two nearby locations (~4 m apart), is given by Figure 6 which shows the snow density profiles, locations of visible ice layers (dashed lines), locations of pink (P) and green (G) microsphere horizons, and the location of the glass shard (S) horizon from sampling conducted at Willie Field in November 1995. Profile A1 (Figure 3) was designated as the reference profile with the glass shard horizon identified at 37.8 cm. Comparing the depth of the glass shard horizon to that of the pink microsphere (38.4 cm) and green microsphere (35.2 cm) horizons in profile B1 (Figure 3), it is apparent that by simply combining the results of the two snow profile produces a sequence which is out of chronological order and indicates that some adjustment must be made. Normalizing profile B1 to the reference profile was accomplished by mapping the reference profile snow density pattern versus depth near 34 cm to a similar pattern near 36 cm in profile B1, resulting in a correction of -2 cm to the depth of the two microsphere horizons in profile B1. Upon further examination of the snow density profiles in Figure 6, it was recognized that ice layers and density profile patterns closer to the surface in both profiles matched but were offset by approximately +5 cm. Using microsphere horizon information from other snow

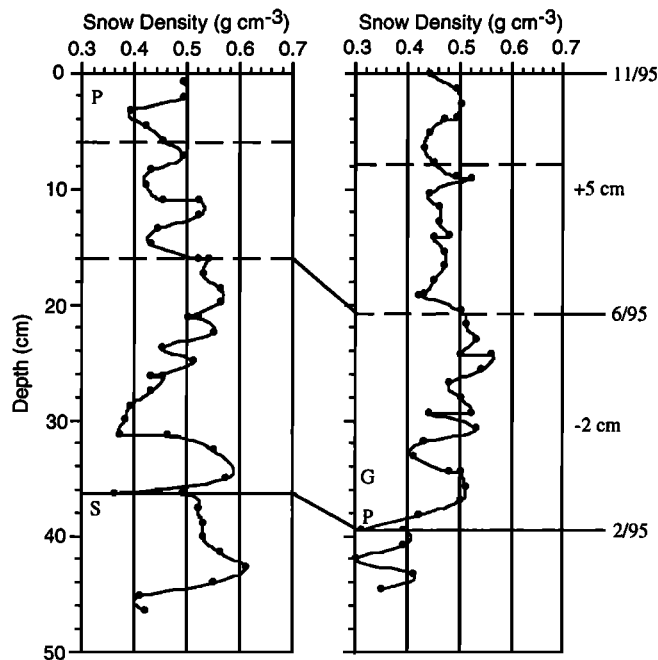


Figure 6. Example of snow pit (left) A1 (reference) and (right) B1 at Willie Field (1995) showing measured snow density with depth and the locations of the visible ice layers (dashed lines), yellow glass shard horizon (S), pink microsphere horizons (P) and green microsphere horizon (G).

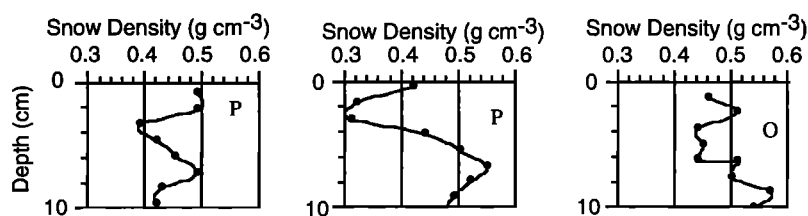


Figure 7. Example of snow pits (left) A1 (reference), (middle) D1, and (right) A2 at Willie Field (1995) showing measured snow density with depth and the locations of the pink microsphere horizons (P) and orange microsphere horizon (O).

profiles, the earlier of these ice layers is estimated to have formed around the beginning of June 1995. This indicates that the accumulation rate for the reference profile is greater than for profile B1 for the first 4 months of the survey period, and the accumulation rate of profile B1 was greater than the reference profile for the remainder of the period. Overall, the net accumulation observed in profile B1 was 3 cm more than the reference profile.

During periods with little snow accumulation, accurate dating of the microsphere horizons identified in different snow pit profiles again must rely on snow density profile patterns and/or visible stratigraphic features to obtain a normalized depth for these horizons. Figure 7 shows the snow density profiles, and locations of pink (P) microsphere horizons at 2.2 cm (reference profile A1) and 3.0 cm (profile D1), and an orange (O) microsphere horizon at 3.9 cm. Profiles A1 and D1 (Figure 3) are separated by a distance of 13 m, and profiles A1 and A2 (Figure 3) are only 1 m apart. Normalizing the depths of the pink horizon found in profile D1 and the orange horizon in profile A2 to the reference profile was based on similar snow density patterns near 2.5 cm in the reference profile, 1.0 cm in profile D1 and 3.4 cm in profile A2. Therefore the normalized pink microsphere horizon depth in profile D1 is 4.5 cm, indicating that the two pink microsphere horizons shown in Figure 7 are from different activations (August 2, 1995, and September 27, 1995). The normalized orange microsphere horizon depth in profile A2 is 3.0 cm, placing it between the two pink microsphere horizons and dating the horizon at August 30, 1995.

Once the microsphere horizons identified from snow pit sampling have been normalized, dates are assigned to the horizons based on the known times of dispersal for each microsphere color, counting forward in time from the glass shard horizon, and counting back in time from the snow surface at the time of snow pit sampling. The ultrasonic snow gauge data, when available, are also used as input in assigning dates to the microsphere horizons. The locations and uncertainty of microsphere horizons along with the date of dispersal to the snow surface at Willie Field and Ferrell during the two field study surveys are shown in Figures 8 and 9, respectively. Figure 8 also includes the ultrasonic snow gauge derived depths at Willie Field (when available) around the time of a scheduled microsphere activation for comparison. Ferrell did not have an ultrasonic snow depth gauge installed on site. The uncertainty in placing the depth of a microsphere horizon ranged from the dimensions of the cuvette sampling tube (1 cm) to several centimeters caused by encountering a mixed horizon, or by observed depth variations of the horizon in different snow pit profiles. The noticeably larger uncertainties in the second survey period at Ferrell (Figure 9) compared to the first survey period are the result of using snow

core slices instead of snow pit cuvette sampling to identify microsphere horizons.

For a more quantitative comparison of accumulation between the two sites, the detailed snow density measurements were used to calculate mass accumulation rate integrated over periods dated by the microsphere horizons, the initial snow surface indicated by the glass shards, or the snow surface height at the time of snow pit sampling. Figure 10 gives the calculated mass accumulation rate for all integration periods at each site during both survey periods. The dashed lines give the weighted mean mass accumulation rate for each survey period. The period-integrated mass accumulation rate increased at Willie Field between periods 1 and 2 (0.59 to 0.64 $\text{kg m}^{-2} \text{d}^{-1}$), and decreased between periods 1 and 2 at Ferrell (0.78 to 0.58 $\text{kg m}^{-2} \text{d}^{-1}$). The weighted mean for the entire study period at Willie Field was 0.61 $\text{kg m}^{-2} \text{d}^{-1}$ and at Ferrell was 0.69 $\text{kg m}^{-2} \text{d}^{-1}$. Although the weighted mean accumulation rate at Ferrell is greater than at Willie Field, the difference in the two mean values is not statistically significant at the 5% level. The integration periods of 14 to 28 days shown in Figure 10 provide some indication of the variability of the short-term mass accumulation rate ranging from 0 to more than 2.0 $\text{kg m}^{-2} \text{d}^{-1}$. Considering both sites, none of the seasons during the study period were found to have consistently low or consistently high mass accumulation rates. In addition, no consistent relationship was found between mass accumulation rate and mean wind speed for the integration periods, implying that high wind speeds do not necessarily reduce the mass accumulation rate in areas with an unlimited upwind supply of mobile snow grains. Differences in the mass accumulation rates at the two sites are more likely governed by differences in the mesoscale precipitation patterns associated with storms moving through the area.

The microsphere horizons and corresponding snow density profile provide an opportunity to relate snow surface height measured by an ultrasonic snow depth gauge with actual mass accumulation rates for individual periods. Data have already been presented showing that snow surface height changes at the snow depth gauge are in good agreement with snow surface height changes at the microsphere dispersal area. To obtain mass accumulation rate from a snow surface height change, a snow density profile must be either known, modeled or assumed. In this case the snow density profile is known at the microsphere dispersal site, and this same profile is assumed for the snow depth gauge site. Two characteristically different snow accumulation periods are examined in Table 4 to quantify the differences in the actual mass accumulation rate determined in the microsphere dispersal area and the estimated mass accumulation rate at the snow depth gauge. The first period (April 12, 1995 to July 5, 1995) is a period with a large snow depth change, and the second period (August 2, 1995 to

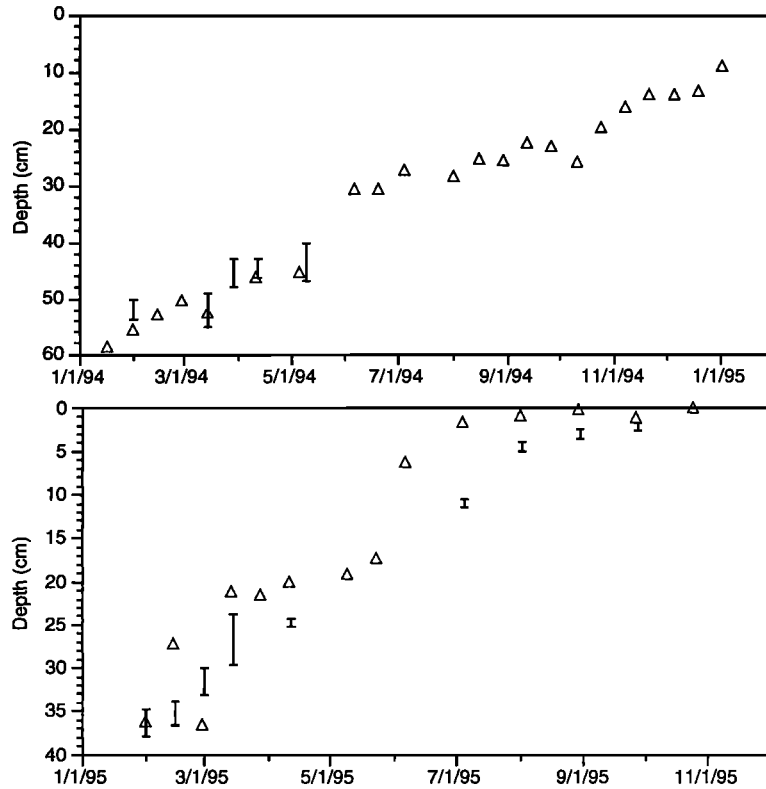


Figure 8. Microsphere horizons identified at Willie Field for the two field periods (top) ending January 28, 1995, and (bottom) ending November 2, 1995, are shown as vertical bars which indicate the date of dispersal and the depth uncertainty in the snow profile. The triangles give the ultrasonic snow depth gauge derived depths around the time of a scheduled microsphere activation (when available).

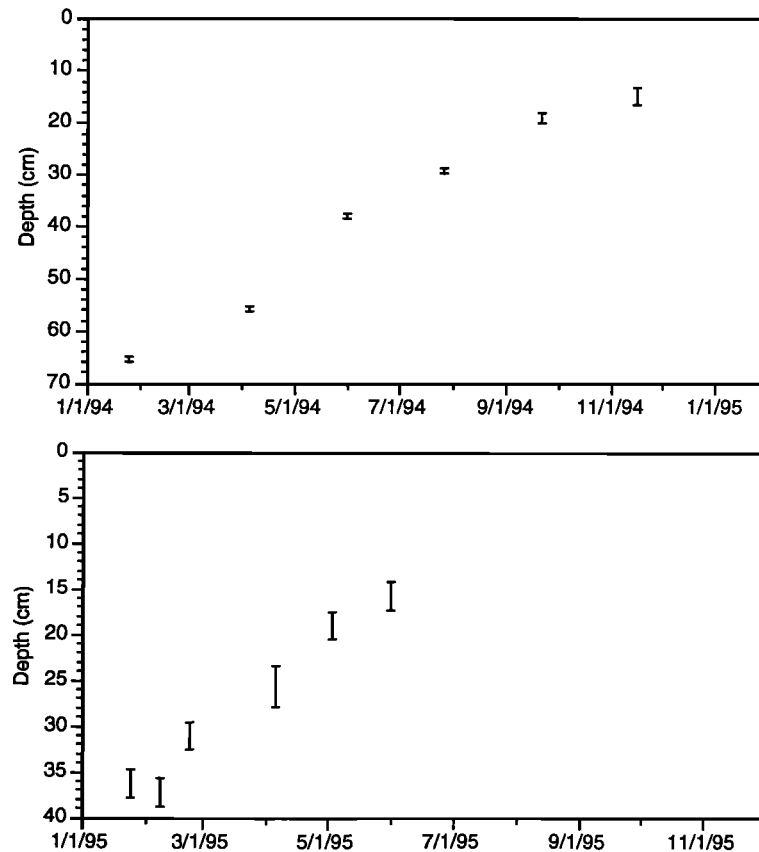


Figure 9. Microsphere horizons identified at Ferrell for the two field periods (top) ending January 23, 1995, and (bottom) ending November 23, 1995, are shown as vertical bars which indicate the date of dispersal and the depth uncertainty in the snow profile.

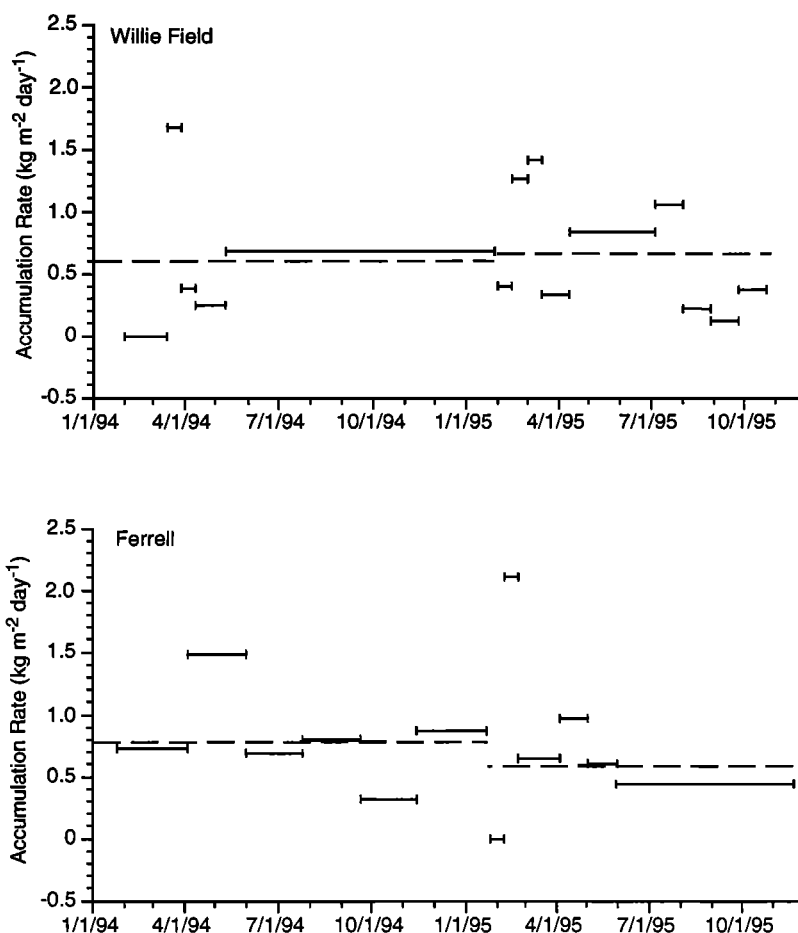


Figure 10. The solid horizontal bars give the mass accumulation rate integrated over periods dated by the microsphere horizons, the glass shard horizon, or the snow surface height at the time of snow pit sampling. The dashed lines indicate the weighted mean mass accumulation rate for each survey period.

November 2, 1995) is a period with a small snow depth change. The length of time covered by both periods allows short-term fluctuations in the snow surface height to be ignored. During the first period the microsphere-derived snow depth change was observed to be 4.6 cm less than that measured by the snow depth gauge, and if the same mean snow density for these layers is assumed, the mass accumulation rate for this period is overestimated by 34%. During the second period, microsphere derived snow depth change was observed to be 3.3 cm greater than that measured by the snow depth gauge, indicating the snow depth gauge underpredicted the mass accumulation rate for this period by 375%. The primary cause of both the overestimations and the underestimations of

mass accumulation by the snow depth gauge is the inability of this instrument to identify when decreases in snow surface height caused by densification and metamorphosis of the snow profile are being offset by the accumulation of new precipitation and/or wind-blown snow.

4. Conclusion

The aim of this research has been to quantify snow accumulation in two windswept ice shelf locations in Antarctica with good time resolution. To accomplish this, a newly developed instrument was used which dispersed colored glass microspheres at fixed intervals to act as time markers

Table 4. Comparison of Measured Mass Accumulation Rates Using Snow Horizons Dated Using Microspheres and Changes in Snow Surface Height Using an Ultrasonic Snow Depth Gauge

Period	Microsphere-Derived Snow Depth Change, cm	Snow Gauge Derived Depth Change, cm	Measured Mean Snow Density, kg m^{-3}	Microsphere-Derived Mass Accumulation Rate, $\text{kg m}^{-2} \text{d}^{-1}$	Snow Gauge Derived Mass Accumulation Rate, $\text{kg m}^{-2} \text{d}^{-1}$
April 12, 1995 to July 5, 1995	13.7	18.3	510.	0.832	1.111
Aug. 2, 1995 to Nov. 2, 1995	4.5	1.2	448.	0.217	0.058

within the growing ice sheet and as wind-blown tracers. The two study sites were located adjacent to automatic weather stations. Both sites were influenced by katabatic outflow winds with one site (Willie Field AWS) having lower average wind speeds than the other (Ferrell AWS). Microspheres chosen for these experiments had a similar terminal settling speed as that of typical snow grains and therefore are a good analog in analyzing snow grain wind erosion. Meteorological data were provided by the automatic weather stations, and precipitation observations were obtained from nearby McMurdo Station. In addition, an ultrasonic snow depth gauge was operated at one of the automatic weather stations.

Weighted mean mass accumulation rates calculated for the two sites showed that Ferrell, with higher overall wind speeds, had the largest accumulation rate. However, the difference in the weighted mean mass accumulation rates was not statistically significant at the 5% level of significance. These results go against the conventional wisdom that the magnitude of the accumulation is generally inversely related to the wind speed magnitude, but additional data to improve statistical confidence are needed to settle this issue. One possible explanation of these results is that the sites have a virtually unlimited upwind supply of erodible snow which replaces snow eroded from the site and that observed accumulation differences are due mainly to differences in mesoscale precipitation patterns affecting the sites. Another important question which should be examined in future research is the effect of even stronger winds on local snow accumulation rate. Over shorter 2 and 4 week integration periods the mass accumulation is highly variable ranging from 0 for periods of either no precipitation or wind erosion to more than $2.0 \text{ kg m}^{-2} \text{ d}^{-1}$ (Ferrell) for a period associated with one or more significant precipitation events. For these shorter periods, no strong correlation between mean wind speed and mass accumulation rate was found, although this analysis with larger data sets is ongoing. In addition, no consistent seasonal trend of mass accumulation was identified in this data set, which is surprising given the influence of sea ice development and retreat on cyclonic storm trajectories. Additional data are needed to confirm this finding as well, but these results point to a large role that wind-blown snow plays in overall net accumulation on the Ross Ice Shelf.

The performance of the ultrasonic snow depth gauge has been assessed using nearby precipitation observations and microsphere-derived snow mass accumulation rates. While most of the snow accumulation events identified by the snow depth gauge were associated with an observed precipitation event, less than half of the observed precipitation events were identified by the snow depth gauge. Although localized precipitation events could explain some of these missed events, high winds accompanying most of the precipitation events likely limited snow accumulation and mask the precipitation event. These results illustrate the limitations of using snow gauge data to identify precipitation events. In addition, snow depth gauge data were shown to significantly over (under) state snow accumulation rates independently

determined using microspheres during periods with large (small) precipitation inputs. This is attributed to the inability of the instrument to identify when decreases in snow surface height caused by densification and metamorphosis of the snow profile are being offset by snow accumulation.

Acknowledgments. The author is indebted to Edward Zeller and Gisela Dreschhoff for sharing their polar experiences and for providing the inspiration and encouragement to pursue the subject of this paper. The author also thanks C. R. Stearns, G. Weidner, and R. Holmes of the Space Science and Engineering Center, University of Wisconsin-Madison for providing the automatic weather station and ultrasonic snow depth gauge data, as well as frequently providing helpful advice. The author gratefully acknowledges the assistance of C. Yess and S. Delfelder in field sampling and laboratory analysis of snow samples, and the helpful suggestions and comments of two anonymous reviewers that improved the text. This investigation was supported by National Science Foundation grants DPP-9218868 and OPP-9417255.

References

- Braaten, D.A., Instrumentation to quantify snow accumulation and transport dynamics at two locations on the Ross Ice Shelf, *Antarct. J. U. S.*, 29(5), 86-87, 1994.
- Braaten, D.A., A new technique to provide high time resolution snowpack dating for stratigraphy and chemistry assessments, *Atmos. Environ.*, 18, 2535-2539, 1995.
- Bromwich, D.H., Snowfall in high southern latitudes, *Rev. Geophys.*, 26, 149-168, 1988.
- Budd, W.F., W.R.J. Dingle, and U. Radok, The Byrd snowdrift project: Outline and basic results, *Studies in Antarctic Meteorology, Antarct. Res. Ser.*, vol. 9, edited by M.J. Rubin, pp. 71-134, AGU, Washington, D. C., 1966.
- Colbeck, S.C., Theory of metamorphism of dry snow, *J. Geophys. Res.*, 88, 5475-5482, 1983.
- Fujii, Y., and K. Kusunoki, The role of sublimation and condensation in the formation of ice sheet surface at Mizuho Station, Antarctica, *J. Geophys. Res.*, 87, 4293-4300, 1982.
- Holmes, R.E., C.R. Stearns, and G.A. Weidner, Antarctic automatic weather stations Field Report: 1996, 19 pp., Space Sci. and Eng. Cent., Univ. of Wis., Madison, 1996.
- Hunter, R.E., Basic types of stratification in small eolian dunes, *Sedimentology*, 24, 361-387, 1977.
- Jacobs, S.S., Is the Antarctic ice sheet growing?, *Nature*, 360, 29-33, 1992.
- Kobayashi, S., Snow transport by katabatic winds in Mizuho Camp Area, East Antarctica, *J. Meteorol. Soc. Jpn.*, 56, 130-139, 1978.
- Kobayashi, S., and T. Ishida, Interaction between wind and snow surface, *Boundary Layer Meteorol.*, 16, 35-47, 1979.
- Maeno, N., K. Nishimura, K. Sugiura, and K. Kosugi, Grain size dependence of eolian saltation lengths during snow drifting, *Geophys. Res. Lett.*, 22, 2009-2012, 1995.
- Mosley-Thompson, E., J.F. Paskievitch, M. Pourchet, A.J. Gow, M.E. Davis, and J. Kleinman, Recent increase in South Pole snow accumulation, *Ann. Glaciol.*, 21, 131-138, 1995.
- Stearns, C.R., and G. Wendler, Research results from automatic weather stations, *Rev. Geophys.*, 26, 45-61, 1988.
- Wendler, G., On the blowing snow in Adelie Land, Eastern Antarctica, in *Glacier Fluctuations and Climate Change*, edited by J. Oerlemans, pp. 261-279, Kluwer Acad., Norwell, Mass., 1989.

D. A. Braaten, Department of Physics and Astronomy, University of Kansas, Lawrence, KS 66045. (e-mail: braaten@kuhub.cc.ukans.edu)

(Received November 20, 1996; revised August 13, 1997; accepted August 15, 1997.)